

CONTROLLED RELEASE FORMULATION OF  
ACTIVE AGENT-ZINC LAYERED HYDROXIDE  
INTERCALATED NANOCOMPOSITE  
FOR PEST CONTROL

 05-4506832  pustaka.upsi.edu.my  Perpustakaan Tuanku Bainun  
Kampus Sultan Abdul Jalil Shah  PustakaTBainun  ptbupsi

ZUHAILIMUNA BINTI MUDA

UNIVERSITI PENDIDIKAN SULTAN IDRIS

2019



05-4506832



pustaka.upsi.edu.my



Perpustakaan Tuanku Bainun  
Kampus Sultan Abdul Jalil Shah



PustakaTBainun



ptbupsi

CONTROLLED RELEASE FORMULATION OF ACTIVE AGENT-ZINC  
LAYERED HYDROXIDE INTERCALATED NANOCOMPOSITE FOR PEST  
CONTROL

ZUHAILIMUNA BINTI MUDA



05-4506832



pustaka.upsi.edu.my



Perpustakaan Tuanku Bainun  
Kampus Sultan Abdul Jalil Shah



PustakaTBainun



ptbupsi

DISSERTATION PRESENTED TO QUALIFY FOR A  
DOCTOR OF PHILOSOPHY (CHEMISTRY)

FACULTY OF SCIENCE AND MATHEMATICS  
UNIVERSITI PENDIDIKAN SULTAN IDRIS

2019



05-4506832



pustaka.upsi.edu.my



Perpustakaan Tuanku Bainun  
Kampus Sultan Abdul Jalil Shah



PustakaTBainun



ptbupsi



Please tick (✓)

Project Paper

Masters by Research

Master by Mixed Mode

PhD

✓

## INSTITUTE OF GRADUATE STUDIES

## DECLARATION OF ORIGINAL WORK

This declaration is made on the .....20.....day of.....09.....20 19.....

## i. Student's Declaration:

I, ZUHAILIMUNA BINTI MUDA, P20151000074, FACULTY OF SCIENCE & MATHEMATICS (PLEASE INDICATE STUDENT'S NAME, MATRIC NO. AND FACULTY) hereby declare that the work entitled CONTROLLED RELEASE FORMULATION OF ACTIVE AGENT-ZINC LAYERED HYDROXIDE INTERCALATED NANOCOMPOSITE FOR PEST CONTROL is my original work. I have not copied from any other students' work or from any other sources except where due reference or acknowledgement is made explicitly in the text, nor has any part been written for me by another person.

Signature of the student

## ii. Supervisor's Declaration:

I ASSOC. PROF. DR. NORHAYATI BINTI HASHIM (SUPERVISOR'S NAME) hereby certifies that the work entitled CONTROLLED RELEASE FORMULATION OF ACTIVE AGENT-ZINC LAYERED HYDROXIDE INTERCALATED NANOCOMPOSITE FOR PEST CONTROL (TITLE) was prepared by the above named student, and was submitted to the Institute of Graduate Studies as a \* partial/full fulfillment for the conferment of DOCTOR OF PHILOSOPHY (CHEMISTRY) (PLEASE INDICATE THE DEGREE), and the aforementioned work, to the best of my knowledge, is the said student's work.

10/10/2019

Date

Signature of the Supervisor

OF. MADYA DR. NORHAYATI HASHIM  
Ketua Jabatan Kemahiran  
Fakulti Sains Dan Matematik  
Universiti Pendidikan Sultan Idris



**INSTITUT PENGAJIAN SISWAZAH /  
INSTITUTE OF GRADUATE STUDIES**

**BORANG PENGESAHAN PENYERAHAN TESIS/DISERTASI/LAPORAN KERTAS PROJEK  
DECLARATION OF THESIS/DISSERTATION/PROJECT PAPER FORM**

Tajuk / Title: CONTROLLED RELEASE FORMULATION OF ACTIVE AGENT-ZINC LAYERED  
HYDROXIDE INTERCALATED NANOCOMPOSITE FOR PEST CONTROL

No. Matrik /Matric's No.: P20151000074

Saya / I : ZUHAILIMUNA BINTI MUDA

(Nama pelajar / Student's Name)

mengaku membenarkan Tesis/Disertasi/Laporan Kertas Projek (Kedoktoran/Sarjana)\* ini disimpan di Universiti Pendidikan Sultan Idris (Perpustakaan Tuanku Bainun) dengan syarat-syarat kegunaan seperti berikut:-

*acknowledged that Universiti Pendidikan Sultan Idris (Tuanku Bainun Library) reserves the right as follows:-*

1. Tesis/Disertasi/Laporan Kertas Projek ini adalah hak milik UPSI.  
*The thesis is the property of Universiti Pendidikan Sultan Idris*
2. Perpustakaan Tuanku Bainun dibenarkan membuat salinan untuk tujuan rujukan dan penyelidikan.  
*Tuanku Bainun Library has the right to make copies for the purpose of reference and research.*
3. Perpustakaan dibenarkan membuat salinan Tesis/Disertasi ini sebagai bahan pertukaran antara Institusi Pengajian Tinggi.  
*The Library has the right to make copies of the thesis for academic exchange.*
4. Sila tandakan ( ✓ ) bagi pilihan kategori di bawah / Please tick ( ✓ ) for category below:-

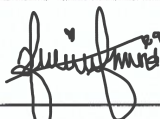
☐ **SULIT/CONFIDENTIAL**

Mengandungi maklumat yang berdarjah keselamatan atau kepentingan Malaysia seperti yang termaktub dalam Akta Rahsia Rasmi 1972. / Contains confidential information under the Official Secret Act 1972


☐ **TERHAD/RESTRICTED**

Mengandungi maklumat terhad yang telah ditentukan oleh organisasi/badan di mana penyelidikan ini dijalankan. / Contains restricted information as specified by the organization where research was done.

☒ **TIDAK TERHAD / OPEN ACCESS**

  
(Tandatangan Pelajar/ Signature)

Tarikh: 10/10/2019

  
(Tandatangan Penyelia / Signature of Supervisor)  
& (Nama & Cop Rasmi / Name & Official Stamp)  
PROF. MADYA DR. NORHAYATI HASMIM  
Ketua Jabatan Kimia  
Fakulti Sains Dan Matematik  
Universiti Pendidikan Sultan Idris

Catatan: Jika Tesis/Disertasi ini **SULIT @ TERHAD**, sila lampirkan surat daripada pihak berkuasa/organisasi berkenaan dengan menyatakan sekali sebab dan tempoh laporan ini perlu dikelaskan sebagai **SULIT** dan **TERHAD**.

Notes: If the thesis is **CONFIDENTIAL** or **RESTRICTED**, please attach with the letter from the organization with period and reasons for confidentiality or restriction.





## ACKNOWLEDGEMENT

In the name of Allah, the Most Gracious and the Most Merciful

Alhamdulillah, all praises to Allah for the strengths and His blessing in completing this thesis. First and foremost I would like to thank my supervisor Assoc. Prof. Dr. Norhayati Hashim, who has shown a large and consistent interest in my project. Our numerous scientific discussions and her many constructive comments have greatly improved this work. Not forgotten, my appreciation to my co-supervisors, Prof. Dr. Illyas Md Isa and Assoc. Prof. Dr. Azlan Kamari for their support and knowledge regarding this topic.

I would like to express my appreciation to the Dean, Faculty of Science and Mathematics, Assoc. Prof. Dr. Haniza Hanim Mohd Zain for the support and help towards my postgraduate affairs. My acknowledgement also goes to all the laboratory assistants and office staffs of Sultan Idris Education University for their co-operation. To Ministry of Education and UPSI, I would like to thank for all afford and support in this research.

My special gratitude goes to my fellow colleagues who have gone through this incredible journey together with me, especially to Ms. Ain, Ms. Hana, Ms. Saleha, and Mrs Shahida. I have learnt so much from all of you.

The last but the most important person, my husband; Mr. Muhamad Suhaidi and my moms; Mrs. Sabariah and Mrs. Fatimah. Thank you for a great love and always being there for me.





## ABSTRACT

This research aimed to synthesis active agent-zinc layered hydroxide intercalated agrochemical nanocomposites namely zinc layered hydroxide-sodium dodecyl sulphate-isoprocab (ZLH-SDS-ISO), zinc layered hydroxide-sodium dodecyl sulphate-propoxur (ZLH-SDS-PRO) and zinc layered hydroxide-sodium dodecyl sulphate-thiacloprid (ZLH-SDS-THI) using ion exchange method for pest control. Surface modification of nanocomposites was performed using chitosan and cellulose acetate. The nanocomposites were characterized using powder x-ray diffraction (PXRD), Fourier transform infrared (FTIR), elemental analysis, thermogravimetric and differential thermogravimetric analysis (TGA/DTG), field emission scanning electron microscope (FESEM), and surface area analysis. The results of PXRD patterns showed the basal spacing in the range of 30.1 Å to 33.1 Å support the successful intercalation process. FTIR spectra for all nanocomposites showed the presence of anion in the interlayer of the nanocomposite. Release study showed that phosphate solution yielded highest percentage release of anion in the range of 90.0 %-97.5 % compared to chitosan and cellulose acetate coated nanocomposite with the range of 77.6 %-87.9 % and 49.1 %-90.0 %, respectively. The results for kinetics study showed that ZLH-SDS-ISO and ZLH-SDS-THI were governed by first order in phosphate solution, meanwhile the release in sulphate and chloride solutions followed the pseudo second order. Whereby, ZLH-SDS-PRO best fitted with pseudo second order in all solutions. All cellulose acetate coated nanocomposites were governed by pseudo second order in all solutions. Chitosan coated ZLH-SDS-ISO (sulphate and chloride) and ZLH-SDS-THI (all solutions) nanocomposites showed best fitted with parabolic, whereas for ZLH-SDS-PRO nanocomposite was best fitted with pseudo second order in all solutions. In conclusion, the nanocomposites were successfully synthesized and the release time for coated nanocomposite was prolonged compared to uncoated nanocomposite. The implication of this research is to improve the cultivation activity by lowering the contamination risk of pesticides in environment.





## FORMULASI PELEPASAN TERKAWAL BAGI NANOKOMPOSIT INTERKALASI AGEN AKTIF- ZINK HIDROKSIDA BERLAPIS UNTUK KAWALAN PEROSAK

### ABSTRAK

Kajian ini bertujuan untuk mensintesis nanokomposit agrokimia interkalasi agen aktif-zink hidroksida berlapis iaitu zink hidroksida berlapis-natrium dodesil sulfat-isoprokarb (ZHB-NDS-ISO), zink hidroksida berlapis-natrium dodesil sulfat-propoxur (ZHB-NDS-PRO) dan zink hidroksida berlapis-natrium dodesil sulfat-thiaklopid (ZHB-NDS-THI) menggunakan kaedah pertukaran ion untuk kawalan perosak. Pengubahsuaian permukaan nanokomposit telah dilakukan menggunakan kitosan dan selulosa asetat. Nanokomposit telah dicirikan menggunakan pembelauan sinar-x serbuk (PXRD), inframerah transformasi Fourier (FTIR), analisis elemen, analisis termogravimetri dan terbitan termogravimetri (TGA/DTG), mikroskop imbasan elektron pancaran medan (FESEM), dan analisis kawasan permukaan. Dapatan pola PXRD nanokomposit menunjukkan jarak dasar dalam julat 30.1 Å hingga 33.1 Å yang menyokong kejayaan proses interkalasi. Spektra FTIR untuk semua nanokomposit menunjukkan kehadiran anion dalam antara lapisan nanokomposit. Kajian pelepasan menunjukkan bahawa larutan fosfat mengeluarkan peratusan pelepasan anion yang tertinggi dalam julat 90.0 %-97.5 % berbanding nanokomposit bersalut kitosan dan selulosa asetat, masing-masing dengan julat 77.6 %-87.9 % dan 49.1 %-90.0 %. Dapatan untuk kajian kinetik menunjukkan bahawa ZHB-NDS-ISO dan ZHB-NDS-THI dalam larutan fosfat dikawal oleh tertib pertama, manakala pelepasan dalam larutan sulfat dan klorida mengikut tertib pseudo kedua. Sementara itu, ZHB-NDS-PRO padanan terbaik dengan tertib pseudo kedua dalam semua larutan. Semua nanokomposit bersalut selulosa asetat dikawal oleh tertib pseudo kedua dalam semua larutan. Nanokomposit bersalut kitosan ZHB-NDS-ISO (sulfat dan klorida) dan ZHB-NDS-THI (semua larutan) menunjukkan padanan terbaik dengan parabola, manakala untuk ZHB-NDS-PRO adalah padanan terbaik dengan tertib pseudo kedua dalam semua larutan. Kesimpulannya, nanokomposit telah berjaya disintesis dan masa pelepasan untuk nanokomposit bersalut telah dipanjangkan berbanding dengan nanokomposit tak bersalut. Implikasi bagi kajian ini adalah untuk menambah baik aktiviti penanaman dengan mengurangkan risiko pencemaran racun perosak dalam alam sekitar.



## TABLE OF CONTENT

	<b>Page</b>
<b>DECLARATION OF ORIGINAL WORK</b>	ii
<b>DECLARATION OF THESIS</b>	iii
<b>ACKNOWLEDGEMENT</b>	iv
<b>ABSTRACT</b>	v
<b>ABSTRAK</b>	vi
<b>TABLE OF CONTENTS</b>	vii
<b>LIST OF TABLES</b>	xv
<b>LIST OF FIGURES</b>	xix
<b>LIST OF ABBREVIATIONS</b>	xxvii
<b>LIST OF APPENDICES</b>	xxix

<b>CHAPTER 1</b>	<b>INTRODUCTION</b>	
	1.1 Pest and Disease	1
	1.2 Controlled Release Formulation	4
	1.3 Zinc Layered Hydroxide	6
	1.4 Problem Statements	8
	1.5 Significance of the Study	14
	1.6 Objectives of Study	14
<b>CHAPTER 2</b>	<b>LITERATURE REVIEW</b>	
	2.1 Nanotechnology	16
	2.2 Nanomaterial	18
	2.3 Nanomaterial in Agriculture	20
	2.4 Layered materials	24
	2.5 Zinc Layered Hydroxide	27
	2.5.1 Properties of Zinc Layered Hydroxide	27



2.5.2 Synthesis Methods of Zinc Layered Hydroxide	31
2.5.3 Application of Zinc Layered Hydroxide	35
2.5.3.1 Wastewater Treatment	35
2.5.3.2 Sensitizers	37
2.5.3.3 Controlled Release Formulation in Biomedical	39
2.5.3.4 Controlled Release Formulation in Agricultural	45
2.6 Coating Materials	48
2.7 Chitosan	49
2.7.1 Properties of Chitosan	49
2.7.2 Application of Chitosan	50
2.8 Cellulose Acetate	51
2.8.1 Properties of Cellulose Acetate	52
2.8.2 Application of Cellulose Acetate	52
2.9 Active Agents of Pesticide	55
2.9.1 Isoprocarb	55
2.9.2 Propoxur	56
2.9.3 Thiachloprid	57

### CHAPTER 3 METHODOLOGY

3.1 Introduction	59
3.2 Chemicals	60
3.3 Instruments	61
3.3.1 Powder x-ray Diffraction (PXRD)	62
3.3.2 Fourier Transform-infrared (FTIR)	63
3.3.3 Elemental Analysis	64
3.3.4 Thermogravimetric Analysis and Differential Thermogravimetric	66

Analysis (TGA/DTG)	
3.3.5 Field Emission Scanning Electron Microscope (FESEM)	66
3.3.6 Surface Area Analysis	67
3.3.7 UV-Vis Spectrophotometer	68
3.4 Synthesizing Zinc Layered Hydroxide Nanocomposite	69
3.5 Synthesizing ZLH Nanocomposite	70
Material Coated Chitosan	
3.6 Synthesizing ZLH Nanocomposite	71
Material Coated Cellulose Acetate	
3.7 Characterization of Layered Material	71
Nanocomposites	
3.8 Release Study of Pesticides	72

## CHAPTER 4 RESULTS AND DISCUSSION

4.1 Introduction	74
4.2 Synthesis and Characterization of Zinc Layered Hydroxide-Sodium Dodecyl Sulphate-Isoprocab Nanocomposite	75
4.2.1 Powder X-Ray Diffraction	75
4.2.2 Fourier Transform Infrared Spectroscopy	78
4.2.3 Spatial Orientation	82
4.2.4 Elemental Analysis	83
4.2.5 Thermal Study	84
4.2.6 Surface Morphology	86
4.2.7 Surface Area Analysis	87
4.3 Synthesis and Characterization of Chitosan Coated Zinc Layered Hydroxide-Sodium Dodecyl Sulphate-Isoprocab Nanocomposite	90
4.3.1 Powder X-Ray Diffraction	90

4.3.2	Fourier Transform Infrared Spectroscopy	93
4.3.3	Thermal Study	96
4.3.4	Surface Morphology	98
4.4	Synthesis and Characterization of Cellulose Acetate Coated Zinc Layered Hydroxide-Sodium Dodecyl Sulphate-Isoprocarb Nanocomposite	100
4.4.1	Powder X-Ray Diffraction	100
4.4.2	Fourier Transform Infrared Spectroscopy	102
4.4.3	Thermal Study	106
4.4.4	Surface Morphology	108
4.5	The Release Study of Isoprocarb from Uncoated and Coated Zinc Layered Hydroxide-Sodium Dodecyl Sulphate-Isoprocarb Nanocomposite	110
4.5.1	The Release Study of Isoprocarb from Zinc Layered Hydroxide-Sodium Dodecyl Sulphate-Isoprocarb Nanocomposite	111
4.5.2	The Release Study of Isoprocarb from Chitosan and Cellulose Acetate Coated Zinc Layered Hydroxide-Sodium Dodecyl Sulphate-Isoprocarb Nanocomposite	115
4.6	Kinetic Study of Isoprocarb from Uncoated and Coated Zinc Layered Hydroxide-Sodium Dodecyl Sulphate-Isoprocarb Nanocomposite	122
4.6.1	Kinetic study of Isoprocarb from Zinc Layered Hydroxide-Sodium Dodecyl Sulphate-Isoprocarb Nanocomposite	123
4.6.2	Kinetic study of Isoprocarb from Chitosan and Cellulose Acetate Coated Zinc Layered Hydroxide-Sodium Dodecyl Sulphate-Isoprocarb Nanocomposite	129



## Sulphate-Isoprocarb Nanocomposite

4.7	Synthesis and Characterization of Zinc Layered Hydroxide-Sodium Dodecyl Sulphate-Propoxur Nanocomposite Chitosan Nanocomposite	139
4.7.1	Powder X-Ray Diffraction	139
4.7.2	Fourier Transform Infrared Spectroscopy	142
4.7.3	Spatial Orientation	146
4.7.4	Elemental Analysis	147
4.7.5	Thermal Study	148
4.7.6	Surface Morphology	150
4.7.7	Surface Area Analysis	151
4.8	Synthesis and Characterization of Chitosan Coated Zinc Layered Hydroxide-Sodium Dodecyl Sulphate-Propoxur Nanocomposite	154
4.8.1	Powder X-Ray Diffraction	154
4.8.2	Fourier Transform Infrared Spectroscopy	156
4.8.3	Thermal Study	159
4.8.4	Surface Morphology	162
4.9	Synthesis and Characterization of Cellulose Acetate Coated Zinc Layered Hydroxide-Sodium Dodecyl Sulphate-Propoxur Nanocomposite	163
4.9.1	Powder X-Ray Diffraction	163
4.9.2	Fourier Transform Infrared Spectroscopy	165
4.9.3	Thermal Study	168
4.9.4	Surface Morphology	171
4.10	The Release Study of Propoxur from Uncoated and Coated Zinc Layered Hydroxide-Sodium Dodecyl	173





### Sulphate-Propoxur Nanocomposite

4.10.1	The Release Study of Propoxur from Zinc Layered Hydroxide-Sodium Dodecyl Sulphate-Propoxur Nanocomposite	173
4.10.2	The Release Study of Propoxur from Chitosan and Cellulose Acetate Coated Zinc Layered Hydroxide-Sodium Dodecyl Sulphate-Propoxur Nanocomposite	177
4.11	Kinetic Study of Propoxur from Uncoated and Coated Zinc Layered Hydroxide-Sodium Dodecyl Sulphate-Propoxur Nanocomposite	183
4.11.1	Kinetic study of Propoxur from Zinc Layered Hydroxide-Sodium Dodecyl Sulphate-Propoxur Nanocomposite	183
4.11.2	Kinetic study of Propoxur from Chitosan and Cellulose Acetate Coated Zinc Layered Hydroxide-Sodium Dodecyl Sulphate-Propoxur Nanocomposite	189
4.12	Synthesis and Characterization of Zinc Layered Hydroxide-Sodium Dodecyl Sulphate-Thiacloprid Nanocomposite	199
4.12.1	Powder X-Ray Diffraction	199
4.12.2	Fourier Transform Infrared Spectroscopy	202
4.12.3	Spatial Orientation	205
4.12.4	Elemental Analysis	206
4.12.5	Thermal Study	207
4.12.6	Surface Morphology	209
4.12.7	Surface Area Analysis	209





4.13	Synthesis and Characterization of Chitosan Coated Zinc Layered Hydroxide-Sodium Dodecyl Sulphate-Thiacloprid Nanocomposite	212
4.13.1	Powder X-Ray Diffraction	212
4.13.2	Fourier Transform Infrared Spectroscopy	215
4.13.3	Thermal Study	217
4.13.4	Surface Morphology	220
4.14	Synthesis and Characterization of Cellulose Acetate Coated Zinc Layered Hydroxide-Sodium Dodecyl Sulphate-Thiacloprid Nanocomposite	221
4.14.1	Powder X-Ray Diffraction	221
4.14.2	Fourier Transform Infrared Spectroscopy	223
4.14.3	Thermal Study	225
4.14.4	Surface Morphology	227
4.15	The Release Study of Thiacloprid from Uncoated and Coated Zinc Layered Hydroxide-Sodium Dodecyl Sulphate-Propoxur Nanocomposite	229
4.15.1	The Release Study of Thiacloprid from Zinc Layered Hydroxide-Sodium Dodecyl Sulphate-Thiacloprid Nanocomposite	229
4.15.2	The Release Study of Thiacloprid from Chitosan and Cellulose Acetate Coated Zinc Layered Hydroxide-Sodium Dodecyl Sulphate-Thiacloprid Nanocomposite	232
4.16	Kinetic Study of Thiacloprid from Uncoated and Coated Zinc Layered Hydroxide-Sodium Dodecyl	237

## Sulphate-Propoxur Nanocomposite

4.16.1	Kinetic study of Thiacloprid from Zinc Layered Hydroxide-Sodium Dodecyl Sulphate-Thiacloprid Nanocomposite	237
4.16.2	Kinetic study of Thiacloprid from Chitosan and Cellulose Acetate Coated Zinc Layered Hydroxide-Sodium Dodecyl Sulphate-Propoxur Nanocomposite	243
4.17	Effect of Single, Binary and Ternary Anion of Sodium Phosphate, Sodium, Sulphate, and Sodium Chloride for the Controlled Release of Nanocomposite	253
4.17.1	Release Study of Isoprocab from ZLH-SDS-ISO, ZLH-SDS-ISO-CHIT, ZLH-SDS-ISO-CA Nanocomposite into Mixture Aqueous Solutions	253
4.17.2	Release Study of Propoxur from ZLH-SDS-PRO, ZLH-SDS-PRO-CHIT, ZLH-SDS-PRO-CA Nanocomposite into Mixture Aqueous Solutions	258
4.17.3	Release Study of Thiacloprid from ZLH-SDS-THI, ZLH-SDS-THI-CHIT, ZLH-SDS-THI-CA Nanocomposite into Mixture Aqueous Solutions	263
<b>CHAPTER 5</b>	<b>CONCLUSION</b>	<b>269</b>
5.1	Recommendation	273
<b>REFERENCES</b>		<b>274</b>
<b>APPENDICES</b>		<b>303</b>



## LIST OF TABLES

Table No.		Page
1.1	List of Pesticide Correspondent to their Chemical Family And Mode of Action	10
2.1	The Previously Reported Method and Anion that Successfully Intercalated into the Interlayer of ZLH	33
2.2	The Previously Synthesized ZLH-Based Nanocomposite, Kinetic Model and their Active Agents in Biomedical Applications	39
2.3	List of Pesticide Intercalated into ZLH and its Kinetic Model in Controlled Release Study	47
2.4	List of Application based on Chitosan-Coated Nanocomposite	50
2.5	List of Application based on Cellulose Acetate-Coated Nanocomposite	53
3.1	List of Chemicals	60
4.1	FTIR Bands for ZLH-SDS, ZLH-SDS-ISO Nanocomposite, And Isoprocab Anion	81
4.2	Compositional Data for Synthesized ZLH-SDS and ZLH-SDS-ISO Nanocomposite	84
4.3	Surface Properties of ZLH-SDS and ZLH-SDS-ISO Nanocomposite	89
4.4	FTIR Bands for ZLH-SDS-CHIT, ZLH-SDS-ISO-CHIT Nanocomposite, and Chitosan	95
4.5	FTIR Bands for ZLH-SDS-CHIT, ZLH-SDS-ISO-CHIT Nanocomposite, and CA	105
4.6	Percentage Release of Isoprocab Anion from ZLH-SDS-ISO Nanocomposite into Various Solutions	114
4.7	Percentage Release of Isoprocab Anion from ZLH-SDS-ISO-CHIT and ZLH-SDS-ISO-CA Nanocomposites into Various Solutions	119
4.8	Rate Constants, Half-life ( $T_{1/2}$ ), and Correlation Coefficients	128



Obtained from the Fitting of the Data of Isoprocارب Release from ZLH-SDS-ISO Nanocomposite into Sodium Phosphate, Sodium Sulphate, and Sodium Chloride Solutions

4.9	Rate Constants, Half-life ( $T_{1/2}$ ), and Correlation Coefficients Obtained from the Fitting of the Data of Isoprocارب Release from ZLH-SDS-ISO-CHIT Nanocomposite into Sodium Phosphate, Sodium Sulphate, and Sodium Chloride Solutions	137
4.10	Rate Constants, Half-life ( $T_{1/2}$ ), and Correlation Coefficients Obtained from the Fitting of the Data of Isoprocارب Release from ZLH-SDS-ISO-CA Nanocomposite into Sodium Phosphate, Sodium Sulphate, and Sodium Chloride Solutions	138
4.11	FTIR Bands for ZLH-SDS, ZLH-SDS-PRO Nanocomposite, and Propoxur Anion	145
4.12	Compositional Data for Synthesized ZLH-SDS and ZLH-SDS-PRO Nanocomposite	148
4.13	Surface Properties of ZLH-SDS and ZLH-SDS-PRO Nanocomposite	151
4.14	FTIR Bands for ZLH-SDS-CHIT, ZLH-SDS-PRO-CHIT Nanocomposite, and Chitosan	159
4.15	FTIR Bands for ZLH-SDS-CA, ZLH-SDS-PRO-CA Nanocomposite, and CA	168
4.16	Percentage Release of Propoxur Anion from ZLH-SDS-PRO Nanocomposite into Various Solutions	176
4.17	Percentage Release of Propoxur Anion from ZLH-SDS-PRO-CHIT and ZLH-SDS-PRO-CA Nanocomposites into Various Solutions	181
4.18	Rate Constants, Half-life ( $T_{1/2}$ ), and Correlation Coefficients Obtained from the Fitting of the Data of Propoxur Release from ZLH-SDS-PRO Nanocomposite into Sodium Phosphate, Sodium Sulphate, and Sodium Chloride Solutions	188
4.19	Rate Constants, Half-life ( $T_{1/2}$ ), and Correlation Coefficients Obtained from the Fitting of the Data of Propoxur Release from ZLH-SDS-PRO-CHIT Nanocomposite into Sodium Phosphate, Sodium Sulphate, and Sodium Chloride Solutions	197
4.20	Rate Constants, Half-life ( $T_{1/2}$ ), and Correlation Coefficients Obtained from the Fitting of the Data of Propoxur Release from ZLH-SDS-PRO-CA Nanocomposite into Sodium Phosphate, Sodium Sulphate, and Sodium Chloride Solutions	198



4.21	FTIR Bands for ZLH-SDS, ZLH-SDS-THI Nanocomposite, and Thiocloprid Anion	204
4.22	Compositional Data for Synthesized ZLH-SDS and ZLH-SDS-THI Nanocomposite	206
4.23	Surface Properties of ZLH-SDS and ZLH-SDS-THI Nanocomposite	210
4.24	FTIR Bands for ZLH-SDS-CHIT, ZLH-SDS-THI-CHIT Nanocomposite, and Chitosan	217
4.25	FTIR Bands for ZLH-SDS-CA, ZLH-SDS-THI-CA Nanocomposite, and CA	224
4.26	Percentage Release of Thiocloprid Anion from ZLH-SDS-THI Nanocomposite into Various Solutions	232
4.27	Percentage Release of Thiocloprid Anion from ZLH-SDS-THI-CHIT and ZLH-SDS-THI-CA Nanocomposites into Various Solutions	235
4.28	Rate Constants, Half-life ( $T_{1/2}$ ), and Correlation Coefficients Obtained from the Fitting of the Data of Thiocloprid Release from ZLH-SDS-THI Nanocomposite into Sodium Phosphate, Sodium Sulphate, and Sodium Chloride Solutions	242
4.29	Rate Constants, Half-life ( $T_{1/2}$ ), and Correlation Coefficients Obtained from the Fitting of the Data of Thiocloprid Release from ZLH-SDS-THI-CHIT Nanocomposite into Sodium Phosphate, Sodium Sulphate, and Sodium Chloride Solutions	251
4.30	Rate Constants, Half-life ( $T_{1/2}$ ), and Correlation Coefficients Obtained from the Fitting of the Data of Thiocloprid Release from ZLH-SDS-THI-CA Nanocomposite into Sodium Phosphate, Sodium Sulphate, and Sodium Chloride Solutions	252
4.31	The Release Order of Isoprocarb from the ZLH-SDS-ISO, ZLH-SDS-ISO-CHIT, ZLH-SDS-ISO-CA Nanocomposites into Various Solutions.	257
4.32	The Accumulated Release (%) of Isoprocarb from the ZLH-SDS-ISO, ZLH-SDS-ISO-CHIT, ZLH-SDS-ISO-CA Nanocomposites into Various Solutions.	258
4.33	The Release Order of Propoxur from the ZLH-SDS-PRO, ZLH-SDS-PRO-CHIT, ZLH-SDS-PRO-CA Nanocomposites into Various Solutions.	261
4.34	The Accumulated Release (%) of Propoxur from the ZLH-	262





SDS-PRO, ZLH-SDS-PRO-CHIT, ZLH-SDS-PRO-CA  
Nanocomposites into Various Solutions.

- |      |  |     |
|------|--|-----|
| 4.35 | The Release Order of Thiacloprid from the ZLH-SDS-THI, ZLH-SDS-THI-CHIT, ZLH-SDS-THI-CA Nanocomposites into Various Solutions.           | 267 |
| 4.36 | The Accumulated Release (%) of Thiacloprid from the ZLH-SDS-THI, ZLH-SDS-THI-CHIT, ZLH-SDS-THI-CA Nanocomposites into Various Solutions. | 267 |



## LIST OF FIGURES

Figure No.		Page
2.1	The interlamellar structure of ZLH (Lee, Choi, & Kim, 2010)	29
2.2	General chemical structure of chitosan	49
2.3	General chemical structure of cellulose acetate	52
4.1	X-ray diffraction pattern of ZLH-SDS, isoprocarb and ZLH-SDS-ISO nanocomposite at 0.001 M, 0.0025M, and 0.005 M concentration of isoprocarb. Inset is the molecular structure of isoprocarb	77
4.2	The FTIR spectra for ZLH-SDS, ZLH-SDS-ISO nanocomposite, and isoprocarb anion	80
4.3	The proposed orientation of isoprocarb and SDS anions intercalated within the ZLH interlayer gallery resulting in the ZLH-SDS-ISO nanocomposite, estimated by Chemoffice software	82
4.4	Thermogravimetric curve for (a) isoprocarb anion, (b) ZLH-SDS and (c) ZLH-SDS-ISO nanocomposite	85
4.5	FESEM images of (a) ZLH-SDS and (b) ZLH-SDS-ISO nanocomposite at 10 k magnification	87
4.6	Adsorption–desorption isotherms of nitrogen gas for (a) ZLH-SDS and (b) ZLH-SDS-ISO nanocomposite	89
4.7	BJH desorption pore size distributions for (a) ZLH-SDS, and (b) ZLH-SDS-ISO nanocomposite	90
4.8	PXRD pattern for chitosan, ZLH-SDS-CHIT, ZLH-SDS-ISO and ZLH-SDS-ISO-CHIT nanocomposites	92
4.9	FTIR spectra for ZLH-SDS-CHIT, ZLH-SDS-ISO-CHIT nanocomposite and chitosan	94
4.10	Thermogravimetric curve for (a) chitosan, (b) ZLH-SDS-CHIT, and (c) ZLH-SDS-ISO-CHIT nanocomposite	97
4.11	FESEM images of (a) chitosan, (b) ZLH-SDS-CHIT, and (c) ZLH-SDS-ISO-CHIT nanocomposite at 10k	99



magnification

4.12	PXRD pattern for CA, ZLH-SDS-CA, ZLH-SDS-ISO and ZLH-SDS-ISO-CA nanocomposites	101
4.13	FTIR spectra for ZLH-SDS-CA, ZLH-SDS-ISO-CA nanocomposite and CA	104
4.14	Thermogravimetric curve for (a) CA, (b) ZLH-SDS-CA, and (c) ZLH-SDS-ISO-CA nanocomposite	107
4.15	FESEM images of (a) CA, (b) ZLH-SDS-CA, and (c) ZLH-SDS-ISO-CA nanocomposite at 10k magnification	109
4.16	Release profile of isoprocab from ZLH-SDS-ISO nanocomposite into 0.1 M, 0.2 M and 0.3 M concentration of aqueous (a) sodium phosphate, (b) sodium sulphate, and (c) sodium chloride solutions	112
4.17	Release profile of isoprocab from ZLH-SDS-ISO-CHIT nanocomposite into 0.1 M, 0.2 M and 0.3 M concentration of aqueous (a) sodium phosphate, (b) sodium sulphate, and (c) sodium chloride solutions	116
4.18	Release profile of isoprocab from ZLH-SDS-ISO-CA nanocomposite into 0.1 M, 0.2 M and 0.3 M concentration of aqueous (a) sodium phosphate, (b) sodium sulphate, and (c) sodium chloride solutions	117
4.19	Fitting of the isoprocab release data from ZLH-SDS-ISO nanocomposite to the (a) zeroth, (b) first, (c) pseudo second order, (d) parabolic diffusion, and (e) Fickian diffusion into various concentration of aqueous sodium phosphate solutions	125
4.20	Fitting of the isoprocab release data from ZLH-SDS-ISO nanocomposite to the (a) zeroth, (b) first, (c) pseudo second order, (d) parabolic diffusion, and (e) Fickian diffusion into various concentration of aqueous sodium sulphate solutions	126
4.21	Fitting of the isoprocab release data from ZLH-SDS-ISO nanocomposite to the (a) zeroth, (b) first, (c) pseudo second order, (d) parabolic diffusion, and (e) Fickian diffusion into various concentration of aqueous sodium chloride solutions	127
4.22	Fitting of the isoprocab release data from ZLH-SDS-ISO-CHIT nanocomposite to the (a) zeroth, (b) first, (c) pseudo second order, (d) parabolic diffusion, and (e) Fickian diffusion into various concentration of aqueous	131

sodium phosphate solutions

- 4.23 Fitting of the isoprocab release data from ZLH-SDS-ISO-CHIT nanocomposite to the (a) zeroth, (b) first, (c) pseudo second order, (d) parabolic diffusion, and (e) Fickian diffusion into various concentration of aqueous sodium sulphate solutions 132
- 4.24 Fitting of the isoprocab release data from ZLH-SDS-ISO-CHIT nanocomposite to the (a) zeroth, (b) first, (c) pseudo second order, (d) parabolic diffusion, and (e) Fickian diffusion into various concentration of aqueous sodium chloride solutions 133
- 4.25 Fitting of the isoprocab release data from ZLH-SDS-ISO-CA nanocomposite to the (a) zeroth, (b) first, (c) pseudo second order, (d) parabolic diffusion, and (e) Fickian diffusion into various concentration of aqueous sodium phosphate solutions 134
- 4.26 Fitting of the isoprocab release data from ZLH-SDS-ISO-CA nanocomposite to the (a) zeroth, (b) first, (c) pseudo second order, (d) parabolic diffusion, and (e) Fickian diffusion into various concentration of aqueous sodium sulphate solutions 135
- 4.27 Fitting of the isoprocab release data from ZLH-SDS-ISO-CA nanocomposite to the (a) zeroth, (b) first, (c) pseudo second order, (d) parabolic diffusion, and (e) Fickian diffusion into various concentration of aqueous sodium chloride solutions 136
- 4.28 PXRD pattern for ZLH-SDS, propoxur anion, and ZLH-SDS-PRO nanocomposite with concentration of 0.0005 M, 0.0010 M and 0.0025 M of propoxur. Inset is the molecular structure of propoxur 141
- 4.29 The FTIR spectra for ZLH-SDS, ZLH-SDS-PRO nanocomposite, and propoxur anion 144
- 4.30 The proposed orientation of propoxur and SDS anions intercalated within the ZLH interlayer gallery resulting in ZLH-SDS-PRO nanocomposite, estimated by Chemoffice software 146
- 4.31 Thermogravimetric curve for (a) propoxur anion, (b) ZLH-SDS, and (c) ZLH-SDS-PRO nanocomposite 149
- 4.32 FESEM images of (a) ZLH-SDS and (b) ZLH-SDS-PRO nanocomposite at 10k magnification 151

4.33	Adsorption–desorption isotherms of nitrogen gas for (a) ZLH-SDS and (b) ZLH-SDS-PRO	153
4.34	BJH desorption pore size distributions for (a) ZLH-SDS, and (b) ZLH-SDS-PRO nanocomposite	153
4.35	PXRD pattern for chitosan, ZLH-SDS-CHIT, ZLH-SDS-PRO and the ZLH-SDS-PRO-CHIT nanocomposites	155
4.36	FTIR spectra for ZLH-SDS-CHIT, ZLH-SDS-PRO-CHIT nanocomposite and chitosan	158
4.37	Thermogravimetric curve for (a) chitosan, (b) ZLH-SDS-CHIT, and (c) ZLH-SDS-PRO-CHIT nanocomposite	161
4.38	FESEM images of (a) chitosan, (b) ZLH-SDS-CHIT, and (c) ZLH-SDS-PRO-CHIT nanocomposite at 10k magnification	162
4.39	PXRD pattern for CA, ZLH-SDS-CA, ZLH-SDS-PRO and the ZLH-SDS-PRO-CA nanocomposites	164
4.40	FTIR spectra for ZLH-SDS-CA, ZLH-SDS-PRO-CA nanocomposite and CA	166
4.41	Thermogravimetric curve for (a) CA, (b) ZLH-SDS-CA, and (c) ZLH-SDS-PRO-CA nanocomposite	170
4.42	FESEM images of (a) CA, (b) ZLH-SDS-CA, and (c) ZLH-SDS-PRO-CA nanocomposite at 10k magnification	172
4.43	Release profile of propoxur from ZLH-SDS-PRO nanocomposite into 0.1 M, 0.2 M and 0.3 M concentration of aqueous (a) sodium phosphate, (b) sodium sulphate, and (c) sodium chloride solutions	175
4.44	Release profile of propoxur from ZLH-SDS-PRO-CHIT nanocomposite into 0.1 M, 0.2 M and 0.3 M concentration of aqueous (a) sodium phosphate, (b) sodium sulphate, and (c) sodium chloride solutions	178
4.45	Release profile of propoxur from ZLH-SDS-PRO-CA nanocomposite into 0.1 M, 0.2 M and 0.3 M concentration of aqueous (a) sodium phosphate, (b) sodium sulphate, and (c) sodium chloride solutions	179
4.46	Fitting of the propoxur release data from ZLH-SDS-PRO nanocomposite to the (a) zeroth, (b) first, (c) pseudo second order, (d) parabolic diffusion, and (e) Fickian diffusion into various concentration of aqueous sodium	185



phosphate solutions

- 4.47 Fitting of the propoxur release data from ZLH-SDS-PRO nanocomposite to the (a) zeroth, (b) first, (c) pseudo second order, (d) parabolic diffusion, and (e) Fickian diffusion into various concentration of aqueous sodium sulphate solutions 186
- 4.48 Fitting of the propoxur release data from ZLH-SDS-PRO nanocomposite to the (a) zeroth, (b) first, (c) pseudo second order, (d) parabolic diffusion, and (e) Fickian diffusion into various concentration of aqueous sodium chloride solutions 187
- 4.49 Fitting of the propoxur release data from ZLH-SDS-PRO-CHIT nanocomposite to the (a) zeroth, (b) first, (c) pseudo second order, (d) parabolic diffusion, and (e) Fickian diffusion into various concentration of aqueous sodium phosphate solutions 191
- 4.50 Fitting of the propoxur release data from ZLH-SDS-PRO-CHIT nanocomposite to the (a) zeroth, (b) first, (c) pseudo second order, (d) parabolic diffusion, and (e) Fickian diffusion into various concentration of aqueous sodium sulphate solutions 192
- 4.51 Fitting of the propoxur release data from ZLH-SDS-PRO-CHIT nanocomposite to the (a) zeroth, (b) first, (c) pseudo second order, (d) parabolic diffusion, and (e) Fickian diffusion into various concentration of aqueous sodium chloride solutions 193
- 4.52 Fitting of the propoxur release data from ZLH-SDS-PRO-CA nanocomposite to the (a) zeroth, (b) first, (c) pseudo second order, (d) parabolic diffusion, and (e) Fickian diffusion into various concentration of aqueous sodium phosphate solutions 194
- 4.53 Fitting of the propoxur release data from ZLH-SDS-PRO-CA nanocomposite to the (a) zeroth, (b) first, (c) pseudo second order, (d) parabolic diffusion, and (e) Fickian diffusion into various concentration of aqueous sodium sulphate solutions 195
- 4.54 Fitting of the propoxur release data from ZLH-SDS-PRO-CA nanocomposite to the (a) zeroth, (b) first, (c) pseudo second order, (d) parabolic diffusion, and (e) Fickian diffusion into various concentration of aqueous sodium chloride solutions 196

4.55	PXRD pattern for ZLH-SDS, thiacloprid anion and ZLH-SDS-THI nanocomposite with concentration of 0.0005 M, 0.0010 M and 0.0025 M of thiacloprid. Inset is the molecular structure of thiacloprid	200
4.56	The FTIR spectra for ZLH-SDS, ZLH-SDS-THI nanocomposite, and thiacloprid anion	203
4.57	The proposed orientation of propoxur and SDS anions intercalated within the ZLH interlayer gallery resulting in ZLH-SDS-THI nanocomposite, estimated by Chemoffice software	205
4.58	Thermogravimetric curve for (a) thiacloprid anion, (b) ZLH-SDS, and (c) ZLH-SDS-THI nanocomposite	208
4.59	FESEM images of (a) ZLH-SDS, and (b) ZLH-SDS-THI nanocomposite at 10k magnification	209
4.60	Adsorption–desorption isotherms of nitrogen gas for (a) ZLH-SDS and (b) ZLH-SDS-THI nanocomposite	211
4.61	BJH desorption pore size distributions for (a) ZLH-SDS, and (b) ZLH-SDS-THI nanocomposite	212
4.62	PXRD pattern for chitosan, ZLH-SDS-CHIT, ZLH-SDS-THI and ZLH-SDS-THI-CHIT nanocomposites	214
4.63	FTIR spectra for ZLH-SDS-CHIT, ZLH-SDS-THI-CHIT nanocomposite and chitosan	216
4.64	Thermogravimetric curve for (a) chitosan, (b) ZLH-SDS-CHIT, and (c) ZLH-SDS-THI-CHIT nanocomposite	219
4.65	FESEM images of (a) chitosan, (b) ZLH-SDS-CHIT, and (c) ZLH-SDS-THI-CHIT nanocomposite at 10k magnification	220
4.66	PXRD pattern for CA, ZLH-SDS-CA, ZLH-SDS-THI and the ZLH-SDS-THI-CA nanocomposites	222
4.67	FTIR spectra for ZLH-SDS-CA, ZLH-SDS-THI-CA nanocomposite and CA	223
4.68	Thermogravimetric curve for (a) CA, (b) ZLH-SDS-CA, and (c) ZLH-SDS-THI-CA nanocomposite	226
4.69	FESEM images of (a) CA, (b) ZLH-SDS-CA, and (c) ZLH-SDS-THI-CA nanocomposite at 10k magnification	228

4.70	Release profile of thiacloprid from ZLH-SDS-THI nanocomposite into 0.1 M, 0.2 M and 0.3 M concentration of aqueous (a) sodium phosphate, (b) sodium sulphate, and (c) sodium chloride solutions	231
4.71	Release profile of thiacloprid from ZLH-SDS-THI-CHIT nanocomposite into 0.1 M, 0.2 M and 0.3 M concentration of aqueous (a) sodium phosphate, (b) sodium sulphate, and (c) sodium chloride solutions	233
4.72	Release profile of thiacloprid from ZLH-SDS-THI-CA nanocomposite into 0.1 M, 0.2 M and 0.3 M concentration of aqueous (a) sodium phosphate, (b) sodium sulphate, and (c) sodium chloride solutions	234
4.73	Fitting of the thiacloprid release data from ZLH-SDS-THI nanocomposite to the (a) zeroth, (b) first, (c) pseudo second order, (d) parabolic diffusion, and (e) Fickian diffusion into various concentration of aqueous sodium phosphate solutions	239
4.74	Fitting of the thiacloprid release data from ZLH-SDS-THI nanocomposite to the (a) zeroth, (b) first, (c) pseudo second order, (d) parabolic diffusion, and (e) Fickian diffusion into various concentration of aqueous sodium sulphate solutions	240
4.75	Fitting of the thiacloprid release data from ZLH-SDS-THI nanocomposite to the (a) zeroth, (b) first, (c) pseudo second order, (d) parabolic diffusion, and (e) Fickian diffusion into various concentration of aqueous sodium chloride solutions	241
4.76	Fitting of the thiacloprid release data from ZLH-SDS-THI-CHIT nanocomposite to the (a) zeroth, (b) first, (c) pseudo second order, (d) parabolic diffusion, and (e) Fickian diffusion into various concentration of aqueous sodium phosphate solutions	245
4.77	Fitting of the thiacloprid release data from ZLH-SDS-THI-CHIT nanocomposite to the (a) zeroth, (b) first, (c) pseudo second order, (d) parabolic diffusion, and (e) Fickian diffusion into various concentration of aqueous sodium sulphate solutions	246
4.78	Fitting of the thiacloprid release data from ZLH-SDS-THI-CHIT nanocomposite to the (a) zeroth, (b) first, (c) pseudo second order, (d) parabolic diffusion, and (e) Fickian diffusion into various concentration of aqueous	247

sodium chloride solutions

- 4.79 Fitting of the thiacloprid release data from ZLH-SDS-THI-CA nanocomposite to the (a) zeroth, (b) first, (c) pseudo second order, (d) parabolic diffusion, and (e) Fickian diffusion into various concentration of aqueous sodium phosphate solutions 248
- 4.80 Fitting of the thiacloprid release data from ZLH-SDS-THI-CA nanocomposite to the (a) zeroth, (b) first, (c) pseudo second order, (d) parabolic diffusion, and (e) Fickian diffusion into various concentration of aqueous sodium sulphate solutions 249
- 4.81 Fitting of the thiacloprid release data from ZLH-SDS-THI-CA nanocomposite to the (a) zeroth, (b) first, (c) pseudo second order, (d) parabolic diffusion, and (e) Fickian diffusion into various concentration of aqueous sodium chloride solutions 250
- 4.82 Release profile of isoprocarb from the a) ZLH-SDS-ISO, b) ZLH-SDS-ISO-CHIT, and c) ZLH-SDS-ISO-CA nanocomposites into mixture aqueous solutions 254
- 4.83 Release profile of propoxur from the a) ZLH-SDS-PRO, b) ZLH-SDS-PRO-CHIT, and c) ZLH-SDS-PRO-CA nanocomposites into mixture aqueous solutions 260
- 4.84 Release profile of thiacloprid from the a) ZLH-SDS-THI, b) ZLH-SDS-THI-CHIT, and c) ZLH-SDS-THI-CA nanocomposites into mixture aqueous solutions 265



## LIST OF ABBREVIATIONS

$\mu\text{m}$	micrometer
2,4-D	2,4-(dichlorophenoxy)acetic acid
2D	2 dimension
4-ASA-ZLH	zinc layered hydroxide-4-aminosalicylate nanocomposite
A549	adenocarcinomic human alveolar basal epithelial cells
CA	cellulose acetate
CHIT	chitosan
CHNO-S	carbon, hydrogen, nitrogen, oxygen and sulphur
EDX	energy dispersive x-ray analysis
$\text{Fe}^{3+}$	ferric
$\text{Fe}^{2+}$	ferrous
FTIR	Fourier transform infrared spectrophotometer
ICP-OES	inductive coupled plasma optical emission spectrometry
KBr	potassium bromide
LDH	layered double hydroxide
LDH-MPP	layered double hydroxide-3-(4methoxyphenyl)propionate nanocomposite
LHS	layered hydroxide salt
LMS	layered metal hydroxide
MPP	3-(4-methoxyphenyl)propionic acid
$\text{NaAsO}_2$	sodium arsenide
$\text{NaClO}_3$	sodium chlorate





nm	nanometer
PHA	polyhydroxyalkanoate
PLAP	pesticides leaching assessment programme
PXRD	powder x-ray diffractometer
SEM	scanning electron microscope
Temp	temperature
TGA/DTG	thermogravimetric analysis and derivative thermogravimetry
Z-CFX	zinc layered hydroxide-ciprofloxacin
ZLH-CPPA	zinc layered hydroxide-2-(3-chlorophenoxy)propionate nanocomposite
ZLH-MPP	zinc layered hydroxide-3-(4methoxyphenyl)propionate nanocomposite
ZLHN	zinc layered hydroxide nitrate
ZLHS	zinc layered hydroxide sulfate
ZLH-SDS-ISO	zinc layered hydroxide-sodium dodecyl sulfate-isoprocab
ZLH-SDS-ISO-CA	zinc layered hydroxide-sodium dodecyl sulfate-isoprocab-cellulose acetate
ZLH-SDS-ISO-CHIT	zinc layered hydroxide-sodium dodecyl sulfate-isoprocab-chitosan
ZLH-SDS-PRO	zinc layered hydroxide-sodium dodecyl sulfate-propoxur
ZLH-SDS-PRO-CA	zinc layered hydroxide-sodium dodecyl sulfate-propoxur-cellulose acetate
ZLH-SDS-PRO-CHIT	zinc layered hydroxide-sodium dodecyl sulfate-propoxur-chitosan
ZLH-SDS-THI	zinc layered hydroxide-sodium dodecyl sulfate-thiacloprid
ZLH-SDS-THI-CHIT	zinc layered hydroxide-sodium dodecyl sulfate-thiacloprid-chitosan
ZLH-SDS-THI-CA	zinc layered hydroxide-sodium dodecyl sulfate-thiacloprid-cellulose acetate



## LIST OF APPENDICES

- A The Examples of Calculations for Proposed Chemical Formula
- B List of Publications and Conference





## CHAPTER 1

### INTRODUCTION



Throughout the last few years, a few serious fungal diseases have attained major interest and put a severe menace to the food supply (Bowers, Bailey, Hebbar, Sanogo, & Lumsden, 2001). Come of the famous epiphytotic disease like black pod, witches' broom, and frosty pod rot that may turn on disastrous losses to the plant cultivation area.

In Brazil, the cocoa beans production has decreased at almost 70 % in just 10 years, predominantly being infected by the fungus, *Moniliophthora perniciosa* which is a fungus responsible for witches' broom disease (Bowers et al., 2001). This fungus has reach long way off Brazil into Peru, Ecuador, Venezuela, and Colombia in South America, and Panama in Central America as well as Caribbean islands of Trinidad





and Tobago (Pereira, 2000; Purdy & Schmidt, 1996). The fungus attacks only tissue (shoots, flowers and pods) that grows actively, causing cacao trees to produce branches without fruit and damaged leaves.

Another disease which called frosty pod rot, is infected by the basidiomycete *Moniliophthora roreri* (Bowers et al., 2001). It is found in South America in all North-western countries. The very first reports of the infection date back to the end of the 19th century, when its intimidating effects devastated Colombian and Ecuadorian plantations. The fungus has at last spread far and wide throughout the region of Latin America, leading to massive production losses and even to the abandonment of their farms (Evans, Stalpers, Samson, & Benny, 1978). The fungus only infects tissues, especially young pods that grow actively. The time between infectious disease and symptoms is approximately 1- 3 months. The most important symptom is the white fungal mat on the surface of the pod (Bowers et al., 2001; Fulton, 1989).

Besides being attacked by fungus and diseases, strawberry, wheat, cocoa, and cotton plantation also having a bad dream toward pests and insects such as mirid. Since 1908, cacao mirids have been identified as a critical pest because of their devastating effect in Ghana (Mahob et al., 2011). The most common species in Ghana and West African countries are *Distantiella theobroma* and *Sahlbergella singularis*. In South-East Asia the *Helopeltis spp.* is responsible for the damage related to mirids while *Monalonion* species are present in South and Central America. Mirid damage on its own, yet it can reduce yields by up to 75 percent if left unattended for three years (Asogwa, Ndubuaku, Ugwu, & Awe, 2010). Cocoa mirids usually permeate the





surface of plant stems, branches and pods, kill the host cells and cause unseen necrotic lesions. Mirids that feed on shoots often kill terminal branches and leaves and cause dieback (Mahob et al., 2011).

Cocoa Pod Borer (CPB), also referred to as cocoa moth, is caused by the *Conopomorpha cramerella* insect. The larvae also feed on *Cynometra cauliflora*, *Dimocarpus longan* (longan), *Litchi chinensis* (lychee), and *Nephelium lappaceum* (rambutan). CPB becomes a real threat in 1841, causing considerable losses in the cocoa industry (Bradley, 1986). CPB is now affects nearly all Indonesian cocoa-producing provinces (Zhang et al., 2014). The rapid spread of CPB and the decrease in cocoa prices also led to decreases in Malaysia's production (Beever, Mumford, Shah, Day, & Hall, 1993; Day, 1989; Zhang et al., 2014). CPB targets both young and mature cocoa pods lead to irregularity and premature ripening. The infection of young pods causes serious losses, as the quantity and quality of the bean is severely affected (Beever et al., 1993).

The fruit and chocolate industry is well aware of the need for a consistent quality supply of this product. It is therefore extremely important that the industry and all its associated institutions continue to support scientific research in core areas such as production, integrated pest and disease management, conservation and improvement of germplasm and biotechnology.





## 1.2 Controlled Release Formulation

Controlled delivery can be defined as a technique or method in which active chemicals are made available at a specified rate and duration to achieve the intended effect (Devi & Maji, 2011). The controlled release system is expected to provide the active ingredient with a constant supply, usually at zero order, by continuously releasing it for a certain period of time (Ummadi, Shravani, Rao, Reddy, & Sanjeev, 2013).

In the past six decades, controlled release technology has progressed. It started in 1952 with the introduction of the first sustained release of the drug delivery system (Park, 2014). The first generation of drug delivery around 1950-1980 focused on the development of sustainable oral and transdermal release systems and the establishment of controlled mechanisms for drug release. Smith Kline & French has introduced the first controlled release formulation (CRF) in 1952 for 12-hour delivery of dextroamphetamine (Dexedrine) (Park, 2014; Wen & Park, 2011). The development of zero-order release systems, self-regulated drug delivery systems, long-term depot formulations and nanotechnology based delivery systems focused on the second generation around 1980-2010. The latter part of the second generation was mainly used to study nanoparticles (Hua, Yang, Wang, & Wang, 2010; Park, 2014). Since then, a basic understanding of controlled drug delivery, such as different mechanisms for the release of drugs, including dissolution, diffusion, osmosis and ion exchange, has been established (Park, 2014). Drug delivery systems have recently received particular interest because they have realized the effective and targeted



delivery of drugs and have minimized the side effects of the traditional drug dosage form in the pharmaceutical sector (Hua et al., 2010).

CRF is well known in pharmaceutical field especially in drug delivery system compared to other field. In agrochemical applications, CRF was originally conceived in the 1970s (Park, 2014; Tu, Hurd, Randall, & Tnc, 2001). Over time, the interest in controlled release has increased and expanded as the economic and social benefits of controlled release technology are realized. The excess amount of pesticide runoff into the surface and groundwater in the agricultural sector has caused water pollution. The CRF can therefore be used to reduce the risks of pollution by reducing the amount of pesticides used for the same activity, thereby reducing the non-target effects (Devi & Maji, 2011; Sopena et al., 2009). CRF is also superior to its counterpart and produces higher yields and improved crop quality (Ahmad, Hussein, Kadir, Sarijo, & Yun Hin, 2015). The use of an efficient controlled release system is one approach to minimizing the use of herbicides. In the CRF, the bulk of the herbicide is trapped in an inert formulation matrix, whereas only a portion of the active ingredient is in an immediately available form. The components trapped in the controlled release matrix are less likely to suffer from environmental losses (Zhenlan, Heng, Bin, & Wanguo, 2009). A number of systems were used to control the release of herbicides. These include alginate encapsulation (Garrido-Herrera, González-Pradas, & Fernández-Pérez, 2006; He et al., 2015) and microencapsulation (He et al., 2015; Li, Dunn, Grandmaison, & Goosen, 1992). More recently, intensive research interests focus on pesticide-layered nanocomposite materials to be used as a controlled pesticide release (Zhenlan et al., 2009). This formulation is also used in active agents such as herbicides, pesticides and regulators for plant growth, in which the active agents are





successfully intercalated into layered materials to produce controlled release formulations (Hussein, Rahman, Sarijo, & Zainal, 2012a).

### 1.3 Zinc Layered Hydroxide

Layered metal hydroxide compounds have attracted a huge interest due to their good intercalation properties. These layered metal hydroxide compounds have a brucite-like structure and their structures and chemical compositions are classified into two types. One is layered double hydroxides (LDHs) and another type is layered basic metal salts or layered hydroxide salt (LHS) (Bae & Jung, 2012; Liu, Zhang, & Zhang, 2015; Miao, Xue, & Feng, 2006). Over the various different two-dimensional lamellar, LHSs have attracted great interest because of their simple synthesis process and their unique anion exchange properties (Miao et al., 2006). The structure of LHS is based on the structure of the mineral brucite ( $\text{Mg}(\text{OH})_2$ ) and consists of hydroxide layers with charge-compensating anions in the interlayer spaces. Positive charges on layers are developed from under-coordination or mixed coordination geometries of interlayer cations. Counter-anions are therefore necessary to stabilize the electrostatic charge on the layers (Bae & Jung, 2012).

Zinc layered hydroxide is the one of categorized under LHS. ZLH consists of only one type of divalent metal cation which is differ from LDH that comprised of two metal cations; either one monovalent or one divalent and one trivalent cations (Ahmad et al., 2016). Recently, ZLH catch huge attention due to versatile properties and their wide technological application. ZLH has high zeta potential, which is 20-30



mV likes to that of LDH, which is a strong driving force to the surface of the cell that prevents the accumulation of inorganic nanoparticle (Hussein, Ghotbi, Yahaya, & Rahman, 2009b; Saifullah, Hussein, Hussein-Al-Ali, Arulselvan, & Fakurazi, 2013). The biocompatibility, controlled released and easier degradation without accumulation gives a significant characteristic of ZLH as well as LDH, which makes them a strong candidate as a drug-delivery system (Saifullah et al., 2013). The appealing aspect of ZLH is their simple synthesis and high anion-exchange capacity comparable to LDH. On that point,  $\text{Zn}(\text{OH})_2$  lamellae represent attractive nanobuilding blocks for production of zinc oxide nanosheets (Demel et al., 2010).

Previous study also prove that ZLH has improves thermal stability of the nanohybrid materials in the thermal decomposition profiles (Bashi, Hussein, Zainal, & Tichit, 2013; Saifullah et al., 2013). This is probably due to barrier effect that preventing the heat to transmit quickly and limiting the continuous decomposition of the nanocomposite (Wei'an, Yu, Luo, & Yue'e, 2003). Thus the transfer rate can be retarded, and the combustion time can be prolonged (Zhang, Kang, & Hu, 2013). LHS thermal decomposition profiles generally consist of two isolated thermal events: (i) loss of hydration water and (ii) release of dehydroxylated water, as well as release of gas from the counter-ions, for example  $\text{NO}_2$  (Hashim et al., 2018),  $\text{Cl}_2$  (Arizaga, 2012),  $\text{CO}_2$  (Bitenc, Marinsek, & Crnjak Orel, 2008),  $\text{SO}_3$  (Machovsky, Kuritka, Sedlak, & Pastorek, 2013) or  $\text{CH}_3\text{COOH}$  (Rajamathi, Britto, & Rajamathi, 2005). In the second stage, the largest percentage of mass losses occurs, while the remaining compounds being metal oxides. This last step is the slowest due to the effects of absorption / adsorption on the remaining layered structures and/or the oxides (Arizaga, Satyanarayana, & Wypych, 2007). Due to the fact that ZLH is a single





metal hydroxide, it is a suitable precursor for upcoming product in which the size of these particles may play a role in determining the properties of the resultant product (Ghotbi, Bagheri, & Sadrnezhad, 2011; Hussein et al., 2009).

The effect of the anion size and its simultaneous controlled release property using zinc-layered hydroxide as the host material can be used as a promising new host delivery system similar to LDHs for controlled release purposes (Hussein, Rahman, et al., 2012b). The previous release study of 2, 4-dichlorophenoxyacetic acid (2, 4-D) from the interlayer 2, 4-dichlorophenoxy acetate-zinc layered hydroxide nanocomposite into an aqueous solution of sodium carbonate reported that the amount release of 2, 4-D from ZLH nanocomposite was higher than Zn/Al-LDH nanocomposite (Bashi et al., 2013, Hussein et al., 2009). This was due to the weaker electrostatic interaction of the anionic 2, 4-D species with ZLH layers than LDH layers (Bashi et al., 2013). LDH nanocomposite may have stronger attraction between LDH and 2, 4-D anions due to higher positive charge involving  $\text{Zn}^{2+}$  and  $\text{Al}^{3+}$  ions. Whereas, ZLH layer only involving  $\text{Zn}^{2+}$  ions that provide a weak attraction towards the 2, 4-D anions, make it easy to be released into the aqueous solution. Both ZLH and LDH have good potential as host lattice for herbicide guest anion in controlled release formulation.

#### 1.4 Problem Statements

In the present day, most of the agricultural activities utilize pesticide in order to boost their production in order to achieve good quality and market requirements to protect



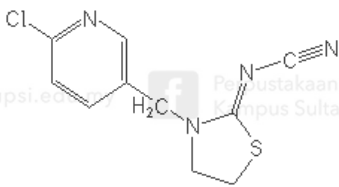
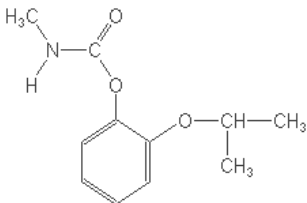
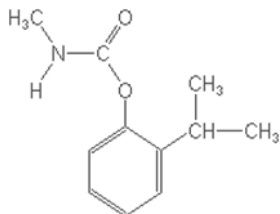
their plant from disease and pest attack. The use of pesticide has shown a remarkable effect in increasing the production for the farmer. For example, the control of diseases and pests in the cocoa belt of Western Nigeria, have increased the cocoa production about 40-50 % by employing the pesticide in cocoa plantation (Idris et al., 2013). In year 2014, Department of Statistics Malaysia press has reported that the production of cocoa in Malaysia has decrease by 3.6 % compared to year 2013 (“Department of Statistics Malaysia press release,” 2014). Idris et al., (2013) reported that, one of the major problems facing cocoa production is pests and diseases outbreak. The effect of pests and diseases reduced crop yield, losses in the value of foreign exchange, reduction in farmer’s income and also reduction in government revenue.

The decline in plant production was affected by many factors such as pest attacks (cocoa mirids, whiteflies, aphids, codling moths, ants and leafhoppers) and diseases (black pod disease, capsids and swollen shoot disease), high cost of inputs (fertilizers, pesticides, and seeds), and shortage of labor (Asogwa et al., 2010; Beevor et al., 1993; Bradley, 1986; Fulton, 1989; Mahob et al., 2011; Rudgard & Butler, 1987; Soberanis et al., 1999). Yield losses attributed to mirids have been reported to be 30-40 % (Asogwa et al., 2010). In 1989, the cocoa moths or cocoa pod borer has contributed to the severe decline of the cocoa industry over a 3-year period in Sabah ranging from £336 to £1128 ha<sup>-1</sup> (assuming a cocoa price of £800 t<sup>-1</sup>) (Beevor et al., 1993). As a solution, various active agent such as thiacloprid, propoxur and isoprocarb has been use to control pest and overcome diseases. Pesticides are rarely used in the way they are synthesized. In addition to the active ingredient, chemicals such as additives are added in order to meet administrative standards without lowering the effectiveness of the active ingredient (Sopena et al., 2009). In view of the negative

role that pest and diseases play in cocoa production, their control has been of utmost importance among agriculturists (Idris et al., 2013). Thiacloprid was applied to control whiteflies, aphids, and codling moths. Whereas, propoxur and isoprocarb used to control ants, gypsy moths, leafhoppers and mollusk (Bakhti & Hamida, 2014; Englert, Bundschuh, & Schulz, 2012; Pandey & Guo, 2014). Table 1.1 shows the structure, chemical family and mode of action of respective pesticides.

Table 1.1

*List of Pesticide Correspondent to their Chemical Family and Mode of Action*

Herbicide	Structure	Chemical family	Mode of action
Thiacloprid		Neonicotinoids	Nicotinic Acetylcholine Receptor agonists/antagonists
Propoxur		Carbamate	Acetylcholine esterase inhibitors
Isoprocarb		Carbamate	Acetylcholine esterase inhibitors

Although, nowadays there are many pesticides and plant growth regulator in the market, the efficiency of these chemical is quite questionable. The use of these

chemical in extensive doses will cause a great impact to the environment. The presence of residual pesticide in soil has many possible causes. Sometimes it is due to aerial treatments applied directly to the plant foliage in order to control pests and diseases, following which approximately 50% of the used product finally deposits in soil. Another case, it occurs by pesticide drift from the host by rain or wind. The pesticide residue may come from excess amount of pesticide applied to the soil and derive from plant residues remaining in the soil after harvest (Sopena et al., 2009). Kamble (2007) has reported that the total percentage abnormalities in pollen mother cells increase with increased in concentration of pesticide on meiosis of *Cannabinus Lin.* The pesticide use also should be environmental friendly and safer for worker (Sopena et al., 2009). The uses of pesticides can also risk human via drinking water. Pesticides are conceived to present a bigger menace because they are highly concentrated in the water supply due to runoff from the agricultural use. The prevalent exposure of the world population to this substance has caused concern over their potential health consequences. Idris et al. (2013) has reported that residue of pesticides has a significant environmental impact on aquatic ecosystems and mammals. These uncontrolled released pesticides may flow into the drainage and irrigation canal that may lead to pollution.

The previous study done by Zafiropoulos et al. (2014) focuses on the long-term effects of repeated low-level exposure to diazinon, propoxur, and chlorpyrifos pesticides on cardiac function in rabbits. It was found that all pesticides tested increased the oxidative stress and oxidative modifications in the genomic DNA content of the cardiac tissues, resulting in cardiac tissue damage and potentially cell death (Zafiropoulos et al., 2014). Lethal cardiac complications leading to death and



various arrhythmias have been reported after organophosphate and/or carbamate poisonings. A recent market study predicts that the global agrochemical market is estimated to reach \$261.9 billion by 2019. But while opportunities abound, concerns about safety and risks remain. From accidental water contamination to colony collapse disorder, people worry about environmental impact. A few issues have caused feedback; most strikingly, the ecological harm produced, including erosion, salinization and flooding of heavily watered soils, aquifer consumption, deforestation and natural defilement because of the unreasonable utilization of pesticides (Sopena et al., 2009).

As a response to these problems, this study will involve the hybridization of the isoprocab, propoxur, and thiacloprid pesticides with zinc layered hydroxide (ZLH). This nanocomposite is deemed to be advantageous and is believed to be released in a controlled manner. The isoprocab, propoxur, and thiacloprid pesticide is poorly-soluble pesticides which are difficult to be intercalating into the interlayer of ZLH. The majority of literatures are only focusing to the anionic pesticides. For poorly water-soluble pesticides, their intercalation is usually dependent on anionic surfactant that forms a hydrophobic region in the gallery (Dekany, Berger, Imrik, & Lagaly, 1997; Pavan, Crepaldi, De A. Gomes, & Valim, 1999). The hydrophobic nature and accessibility of the interlayer region of ZLH is helpful for adsorption of target pesticide molecules. In the previous study, Liu et al., (2015) have developed a novel method to make chlorpyrifos (CPF) adsorb into the interlayer of zinc hydroxide nitrate (ZHN) intercalated with dodecylbenzenesulfonate (DBS). The cationic and anionic surfactants interact to form neutral micelles, leaving the ZLH free to capture the desired anion. Since the interlayer spacing in the starting materials





for this procedure is already quite large, this method offers particular promise for the incorporation of bulky anions (Auerbach, Carrado, & Dutta, 2004).

Therefore, this research aims to intercalate pesticides (isoprocab, propoxur, and thiacloprid) into the interlayer of ZLH modified with sodium dodecyl sulfate (SDS) and study the controlled release of those active agents. Those layered material nanocomposite also will be coated with chitosan/cellulose acetate in order to control the rate of pesticide release, sustain the duration of the pesticide release and targeting the release of the pesticide to a specific part of the tree. Chitosan, the deacetylated derivative of chitin is one of the most abundant naturally occurring polysaccharide and possess immense potential as a packaging material owing to its biodegradability, biocompatibility and antimicrobial activity (Mathew & Abraham, 2008). Whereas, cellulose acetate (CA) is the classic membrane material used by the pioneers of modern membrane technology to create asymmetric membranes. It has been widely applied in the biomedical, pharmaceutical, and agricultural fields. In many of these applications CA is extremely attractive due to its low price, good biodegradability, and nontoxicity (Wu & Liu, 2008). Therefore, the intercalation of isoprocab, propoxur, and thiacloprid pesticides into the interlayer of zinc layered hydroxide-sodium dodecyl sulfate (ZLH-SDS) coated chitosan/cellulose acetate would be an ideal slow-release formulation and believed to be crucial for the continued good agricultural practice in plant cultivation.

## 1.5 Significance of the Study

The study of pesticide formulation will be a significant endeavor to obtain a high biological effectiveness, throughout the time required to control harmful weeds. This study will also be beneficial in promoting good work environment by ensuring safer use of pesticide by workers and users. For the plantation industry and business practitioners, the use of pesticide formulation will save the cost by reducing the amount of chemical use for agrochemical activities. Sustainable cocoa will not only help the cocoa and chocolate manufacturers maintain a constant and reliable supply of raw material, but it also will move small holder farmers into a more favorable economy. Moreover, this study will lower the environmental risk factors by avoiding excess use of herbicide to the crops. Consequently, this research might offer some information for future researchers of physical and chemical properties of the active agent used. Their compatibility will conduct future research to formulate new formulation with better performance.

## 1.6 Objectives of Study

The objective of this study is as below:

- a) to synthesis zinc layered hydroxide-sodium dodecyl sulfate-isoprocab (ZLH-SDS-ISO), zinc layered hydroxide-sodium dodecyl sulfate-propoxur (ZLH-SDS-PRO), and zinc layered hydroxide-sodium dodecyl sulfate-thiacloprid (ZLH-SDS-THI) nanocomposites via ion exchange method.

- b) to synthesis layered material-pesticide nanocomposites coated with chitosan/cellulose acetate.
- c) to study the physicochemical properties of layered material-pesticide nanocomposites using PXRD, FTIR, CHNO-S, ICP-OES, TGA/DTG, FESEM, and BET analysis.
- d) to study the controlled release behavior of pesticide from the interlayer of layered material-pesticide nanocomposites and coated nanocomposites.
- e) to compare the release behavior of pesticide from the interlayer of layered material-pesticide nanocomposite and coated nanocomposite into sodium phosphate, sodium, sulfate, and sodium chloride solutions.
- f) to study the effect of single, binary and ternary anion of sodium phosphate, sodium, sulfate, and sodium chloride for the controlled release of layered material-pesticide nanocomposite.